ISBN: 978-3-95450-231-8 ISSN: 2673-5490 doi: 10.18429/JACoW-IPAC2023-WEODB3

UNDERSTANDING THE BEAM QUALITY REQUIREMENT FOR HIGH ENERGY ELECTRON MICROSCOPY*

Y. Wang†, R. Li, X. Li, et al., Tsinghua University, 100084 Beijing, China

Abstract

Commercial electron microscopes with a few hundred keV energy are fundamental tools for understanding the micro- to nano-scale world. One of the frontiers in electron microscopy development is to push the beam energy to MeV range to achieve improved lateral resolution for thick samples. Here we show the theoretical and preliminary experimental analysis of the electron beam quality required in the imaging and diffraction processes with different beam energy. By correlating the diffraction and imaging modalities, we use the focused beam scheme to characterize the beam emittance of a 200 keV TEM. The quantitative correlation between the beam quality and the obtained image resolution are established. This work demonstrates a characterization technique for electron microscopy and provides a guidance for designing a MeV electron diffraction and imaging beamline.

INTRODUCTION

Electron beams and X-ray are two fundamental probes for understanding the micros-cale world on ultrafast time scales. Compared with X-ray, MeV electron beams can achieve higher spacial resolution with a shorter de Broglie wavelength, while the cross section is larger and the sample damage is smaller. Therefore, electrons are favorable for probing thin films, surfaces and gases [1] [2] [3]. However, due to aberrations, space charge forces and energy spread during emission process, the achievable spatial resolution is far less than the theoretical resolution determined by de Broglie formula for UEMs. In most of the UED and UEM devices, the relationship between beam quality and imaging resolution is still unclear. In this work, we carried out experimental characterization of the beam emittance, image resolution and their correlation under various operation configurations of a commercial TEM. The results aim at establishing the connections between the TEM and accelerator communities for describing and quantifying beam properties and controls, as well as provide a guidance for designing an accelerator-based high energy electron microscope.

METHODS

There are several concepts being used to quantify the imaging resolution in a TEM. These commonly used definitions and their connections are illustrated in Fig. 1.

The spacial resolution is usually defined by the full width at half maximum (FWHM) of the point spread function (SPF), in the reciprocal coordinate where the modulated transfer function (MTF) decays to half of its original intensity (MTF_{50}). The two definitions are unified by Fourier transformation [4]. Their relationship can be written as Eq. (1)

$$\mathrm{PSF_{FWHM}MTF_{50}} = \frac{1}{2} \tag{1}$$

For thin specimens, the factors affecting the achievable resolution include the environment vibration, electronic noises, Airy diffraction from apertures, lens aberration and the limited pixel size of the detector. As shown by previous studies, the resolution limits affected by the spherical aberration, chromatic aberration and detector can be derived from their contributions to the MTF envelop, as shown in Eq. (2) [5] [6].

$$\begin{aligned} E_{\mathrm{sph}}(u) &= \exp\left[-\left(\frac{\pi\alpha}{\lambda}\right)^2\left(C_{\mathrm{s}}\lambda^3u^3+\Delta f\lambda u\right)^2\right] \\ E_{\mathrm{chr}}(u) &= \exp\left[-\frac{1}{2}(\pi\lambda\delta)^2u^4\right] \\ \delta &= C_{\mathrm{c}}\left[4\left(\frac{\Delta I_{\mathrm{obj}}}{I_{\mathrm{obj}}}\right)^2+\left(\frac{\Delta E}{V_{\mathrm{acc}}}\right)^2+\left(\frac{\Delta V_{\mathrm{acc}}}{V_{\mathrm{acc}}}\right)^2\right]^{\frac{1}{2}} \\ E_{\mathrm{det}}(u) &= \exp\left[-\frac{1}{2}\pi^2P^2u^2\right] \end{aligned} \tag{2}$$

u denotes the reciprocal coordinate, ΔI_{obj} denotes the lens current jitter, ΔE denotes the intrinsic energy spread during the emission process, ΔV_{acc} denotes the jitter of the accelerating voltage, and P denotes the effective pixel size. The overall effect of the above mentioned factors are combined by convolution in real space.

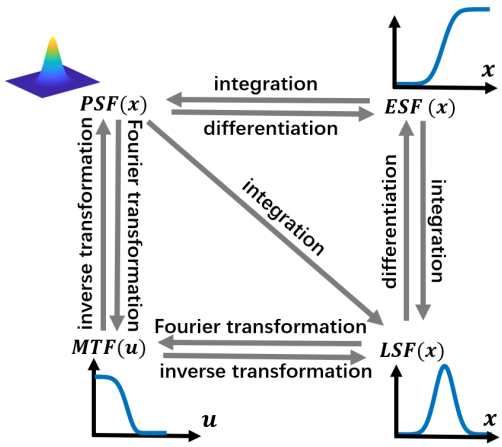

Figure 1: Relationship between point spread function (PSF), edge spread function (ESF), line spread function (LSF) and modulated transfer function (MTF). Label "x" on axis denotes a real space function. Label "u" on axis denotes a reciprocal space function.

* TSINGHUA UNIVERSITY INITIATIVE SCIENTIFIC RESEARCH PROGRAM NO. 20197050028.
† wya20@mails.tsinghua.edu.cn

ISBN: 978-3-95450-231-8 ISSN: 2673-5490 doi: 10.18429/JACoW-IPAC2023-WEODB3

EXPERIMENTS AND RESULTS

We use an FEI Tecnai G^{2}20 TEM to further investigate the relationship between beam parameters and imaging resolution in experiment. The spherical and chromatic aberrations of the objective lens are around 2 mm. The effective pixel size is 0.31 nm. The energy spread is around 0.7 eV, corresponding to a relative energy spread of 3.5×10^{-6}. By switching different modes, the beam waist profile is obtained in both imaging mode and diffraction mode, corresponding to the real space distribution and reciprocal space distribution of the beam respectively. Fig. 2 shows the experimental setup for emittance measurement. Fig. 3 shows the distribution of the main beam in real and reciprocal space.

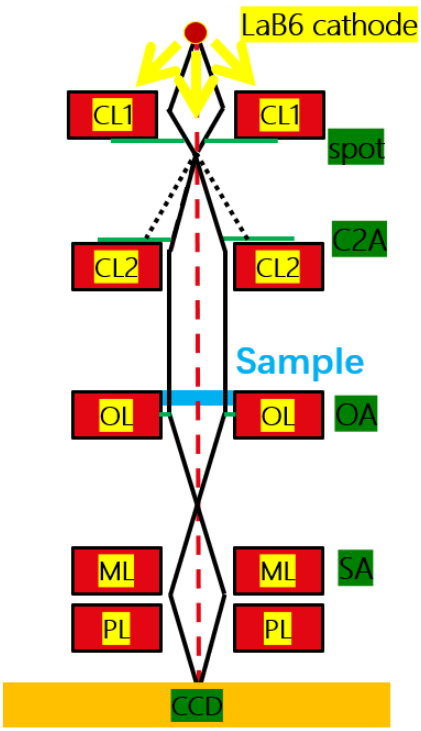

Figure 2: The beam path diagram of a FEI Tecnai G20 TEM. CL1: condenser lens 1, CL2: condenser lens 2, OL: objective lens, ML: middle lens, PL: projector lens, spot: aperture after CL1, C2A: CL2 aperture, OA objective aperture, SA: selective aperture.

Four beam conditions are tested by adjusting the "spot" and "C2A" parameter, which correspond to changing the bunch charge and condenser lens aperture size. The four measured beam profile and emittance are listed in Table 1.

Imaging mode

A gold shadowed polystyrene latex sample is used to test the imaging resolution limit. We first obtain a series of images on the same sample spot by shifting the beam position. The two adjacent images are added and then Fourier transformed to form interferometric fringes. The interference

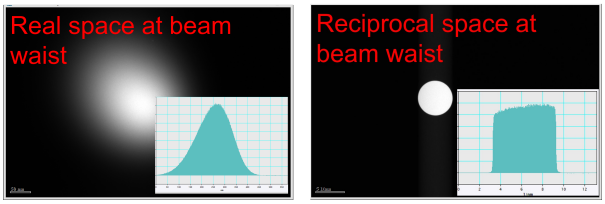

Figure 3: Beam waist profile in reciprocal space (left) and real space (right). The insets on the lower right show the measured intensity distributions of the profiles.

Table 1: Measured beam sizes and divergent angles under different beam optic settings. The electron energy is 200 keV, with $\beta\gamma = 0.97$.

spot	C2A	x(FWHM)	α	ε_n
1	150 μm	180 nm	15 mrad	2.63 nm · rad
2	150 μm	139 nm	15 mrad	2.02 nm · rad
3	150 μm	105 nm	15 mrad	1.51 nm · rad
4	150 μm	70 nm	15 mrad	1.00 nm · rad

limit is obtained as the resolution limit of the image. Fig. 4 shows the structure of the gold shadowed sample, the Fourier transformation of the added images and the data processing procedure. Given the resolution limit where MTF falls to zero, the MTF_{50} can then be deduced from the analytical expression in Eq. (2) and thus $\mathrm{PSF}_{\mathrm{FWHM}}$ can be derived from Eq. (1).

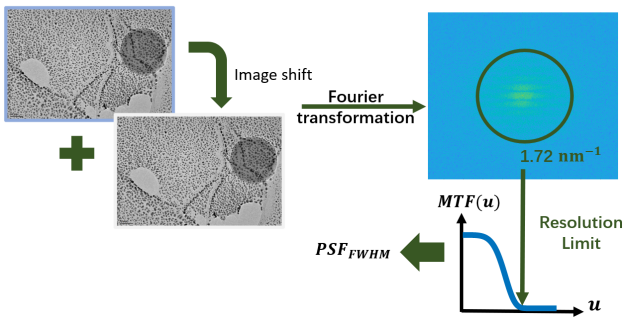

Figure 4: Local folding of the single-layer MoS_2 with its ESF and PSF.

By altering the CL2 (condenser lens 2) current and C2A (CL2 aperture), a series of imaging resolutions are obtained from a relatively wide range of divergent angles. Fig. 5 shows how the resolution limit changes with divergent angle. The dots are experimental results.

The theoretical resolution limit can be obtained using Eq. (2), as is shown in the blue solid line in Fig. 5. For larger divergent angles, the experimental results fit well with our theory. Using the relationship in Eq. (1), the theoretical resolution defined by $\mathrm{PSF}_{\mathrm{FWHM}}$ can be deduced, as is shown in red solid line.

Given the resolution of a commercial TEM, the achievable resolution of MeV electron devices can be estimated. For

ISBN: 978-3-95450-231-8 ISSN: 2673-5490 doi: 10.18429/JACoW-IPAC2023-WEODB3

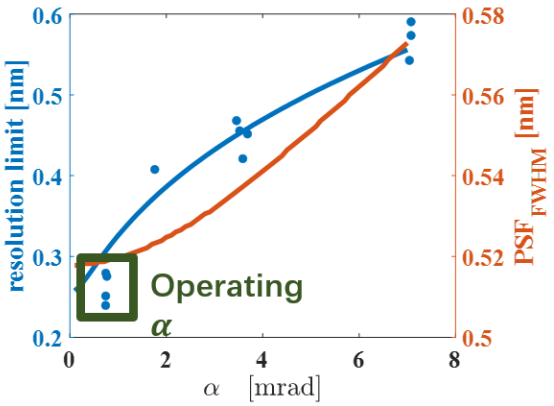

Figure 5: Resolution limit v.s. divergent angle on sample. The dots are the measured resolution limits. The green box shows the typical operating divergent angles in high-resolution TEM mode. The blue solid line indicates the theoretical resolution limit and the red solid line indicates the $\mathrm{PSF_{FWHM}}$ derived from the resolution limit.

a 3-MeV electron beam, the divergent angle is 0.5 mrad on sample, corresponding to an effective angle of $\beta\gamma\alpha \approx$ 3.5 mrad with the same normalized emittance and spot size on sample. For MeV accelerators, the chromatic aberration becomes the dominant factor that limits the resolution as the intrinsic energy spread increases according to $E_{\mathrm{chr}}(\mathbf{u})$ in Eq. (2). Fig. 6 shows how the resolution changes with the energy spread $\Delta E_k/E_k$ using Eq. (2) and Eq. (1).

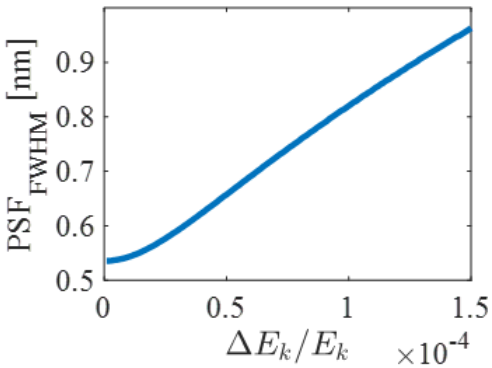

Figure 6: Resolution v.s. energy spread.

However, in a typical 50-Hz photo-cathode electron gun, the dose rate is around 0.01 e/Å^{2}s, far less than the dose rate of 2 e/Å^{2}s in commercial TEMs, meaning that it would take 200 times longer to capture a single frame. Under such conditions, the resolution limit is also affected by shot-to-shot jitters and sample drift during long-term exposure. In our experiment, the sample drift is 0.036 nm/s, which means that an additional 0.72 nm resolution limit is induced in 200-second, long-time exposure. So electron sources with higher repetition frequency is demanded for high-resolution imaging.

Diffraction mode

According to the geometry of diffraction, the lattice spacing is $d = \frac{L\lambda}{D}$, where D denotes the distance between the diffraction point and the center at the detector screen. The reciprocal spacial resolution concerning energy spread can be written as $\frac{\sigma_g^2}{\bar{g}^2} = \frac{\sigma_\lambda^2}{\bar{\lambda}^2} + \frac{\sigma_D^2}{\bar{D}^2}$, where g is the reciprocal coordinate and σ_D is the diffraction spot size on the detector. Since $\frac{\sigma_\lambda}{\lambda} \ll \frac{\sigma_D}{D}$, the reciprocal resolution can be simplified as $\sigma_g \approx \frac{\sigma_D}{\lambda L}$. In diffraction mode, the beam requirements is less restricted. Comparing the TEM diffraction pattern of MoS_2 with MeV diffraction of a single crystal Si in Fig. 7, σ_D could be a limiting factor that somehow constrains the relative strength of keV versus MeV in the spatial domain.

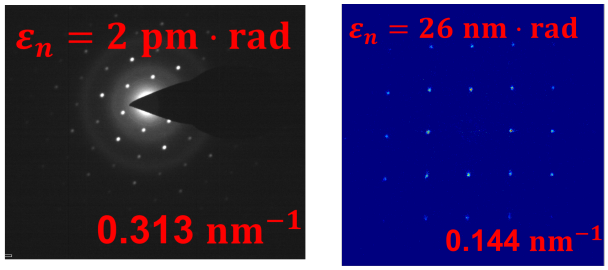

Figure 7: Diffraction of a MoS_2 (left) by TEM and a single crystal Si (right) by UED. The normalized emittances are 2 pm · rad and 26 nm · rad, and the corresponding reciprocal resolutions are 0.313 nm^{-1} and 0.144 nm^{-1} respectively.

CONCLUSIONS

In this study the normalized emittance of a typical commercial TEM is measured using direct phase-space mapping. The resolutions under a wide range of divergent angles for TEM imaging is tested and the results can give estimations for the resolution of MeV electron sources under the same imaging system. Our next goal is to achieve imaging resolution under 1 nm on MeV devices.

ACKNOWLEDGMENT

This work is supported by Tsinghua University Initiative Scientific Research Program No. 20197050028.

REFERENCES

[1] A. H. Zewail, "Four-Dimensional Electron Microscopy", *Science.*, 328.5975(2010):187-193. doi: 10.1126/science.1166135

[2] Sciaini, Germán, and R. J. D. Miller, "Femtosecond electron diffraction: heralding the era of atomically resolved dynamics", *Reports on Progress in Physics.*, 74.9(2011):96101-96136(36). doi: 10.1088/0034-4885/74/9/096101

[3] D. Filippetto *et al.*, "Ultrafast electron diffraction: Visualizing dynamic states of matter", *Reviews of Modern Physics.*, 94.4(2022):045004(60). doi: 10.1103/RevModPhys.94.045004

ISBN: 978-3-95450-231-8 ISSN: 2673-5490 doi: 10.18429/JACoW-IPAC2023-WEODB3

[4] Z. He *et al*., "Spatial resolution and image processing for pinhole camera-based X-ray fluorescence imaging:a simulation study", *NUCL SCI TECH.*, 33.5(2022):19. doi: 10.1007/s41365-022-01036-8

[5] D. B. Williams and C. B. Carter, "High-Resolution TEM" *Transmission electron microscopy: a textbook for materials science*, Plenum Press, 1996, pp. 483-509.

[6] V. Dyck et al., "Ultimate resolution and information in electron microscopy: general principles", *Ultramicroscopy.*, 47.1-3(1992):266-281. doi: 10.1016/0304-3991(92)90202-U